CHAPTER 6

Corrosion of steel reinforcement

C. Andrade
Institute of Construction Science 'Eduardo Torroja', CSIC, Madrid, Spain.

1 Principles of corrosion

Concrete is the most widely used construction material in the world. Many kinds of materials, elements and structures are fabricated with cement-based mixes. Reinforced concrete was industrially developed at the beginning of the 20th century, and it has stimulated tremendous developments in housing and infrastructures.

Reinforced and prestressed concrete represents a very successful combination of materials, not only from a mechanical point of view but also from a chemical perspective, because the hydrated cement is able to provide to the steel an excellent protection against corrosion. This chemical compatibility allows for the composite behaviour of reinforced concrete and is the basis of its high durability.

The composite action occurring in the steel–concrete bond may be unlimited in time while steel remains passive. The study of the conditions leading to reinforcement corrosion is then of high importance because corrosion may significantly affect the load-bearing capacity of reinforced or prestressed concrete.

The natural state of metals is their oxidized state. Metals can be found in nature in the form of oxides, carbonates, sulphates, etc. (minerals). In a pure state only the so-called 'noble' metals can persist in contact with the environment without undergoing oxidation. For the practical use of a metal, a certain energy is invested in its reduction from the natural mineral state. The metal then presents the tendency to liberate this energy to attain its lower energy state. The process by which a metal returns to its mineral state is known as 'corrosion'. Corrosion is therefore the process by which the metal passes from its metallic state at 'zero' valence to its oxidized state liberating electrons. For iron it can be simply written as:

$$Fe \rightarrow Fe^{2+} + 2e^{-}$$

WIT Transactions on State of the Art in Science and Engineering, Vol 28, © 2007 WIT Press
www.witpress.com, ISSN 1755-8336 (on-line)
doi:10.2495/978-1-84564-032-3/06

The electrons are transferred to other substances (oxygen, carbonate, sulphate, etc.) in order to become a neutral substance.

The mechanisms for the transfer of electrons from the metal to another substance can basically occur in two manners: directly or through an aqueous solution. The former is produced at high temperatures where water cannot exist in liquid form, while *aqueous corrosion* is the most common mechanism and it develops at normal temperatures.

Corrosion in the presence of liquid water occurs by an electrochemical mechanism [1]. Chemical reactions and redox processes occur simultaneously. Thus, metallic zones with different electrical potential due to the metal being in contact with a heterogeneous (in concentration) electrolyte or due to heterogeneities in the metal itself are the driving force of chemical reactions involving the exchange of electrons. The process occurs as in a battery where the oxidation of the metal takes place in the anodic zone, as shown in the first reaction, and a reduction takes place in the cathodic zone. For the case of neutral and alkaline electrolytes, the most common cathodic reaction is:

$$O_2 + 4e^- + 2H_2O \rightarrow 4OH^-$$

Therefore the electrons liberated in the anode circulate through the metal to the cathodic zones where they are consumed inducing the reduction of a substance (e.g. oxygen in the second reaction). The final corrosion product would be $Fe(OH)_2$, $Fe(OH)_3$ or some oxyhydroxides derived from them.

For the case of acid solutions the most common cathodic reaction in the reduction of protons

$$2H^+ + 2e^- \rightarrow H_2\uparrow \text{ (gas)}$$

Figure 1 shows the development of the corrosion cell and illustrates the need to have a continuous 'circuit' for the corrosion to progress, as in the case of batteries. The elements of a corrosion cell in aqueous-type corrosion are:

1. the anode, where the metal is dissolved;
2. the cathode, where a substance is reduced and takes up the electrons liberated by the metal during its oxidation;
3. continuity across the metal between anode and cathode;
4. continuity across the electrolyte for the chemical substances to move and become neutral.

The lack of electrolyte or of metal connexion will stop the corrosion and the development of any anodic or cathodic zone.

1.1 Corrosion morphology

The corrosion may progress by a uniform dissolution of the whole surface (Fig. 2a) or by a local attack which, when it is very localized, is called 'pitting' corrosion (Fig. 2b). It may also progress at the microscopic level when it is called 'inter- or trans-granular' (Fig. 2c) attack as metal grains are very locally affected.

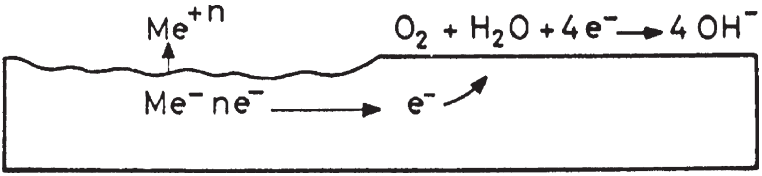

Figure 1: The metal dissolves in the anodic zones releasing metal ions and electrons. The latter are consumed in the cathodic zones reducing another substance such as oxygen.

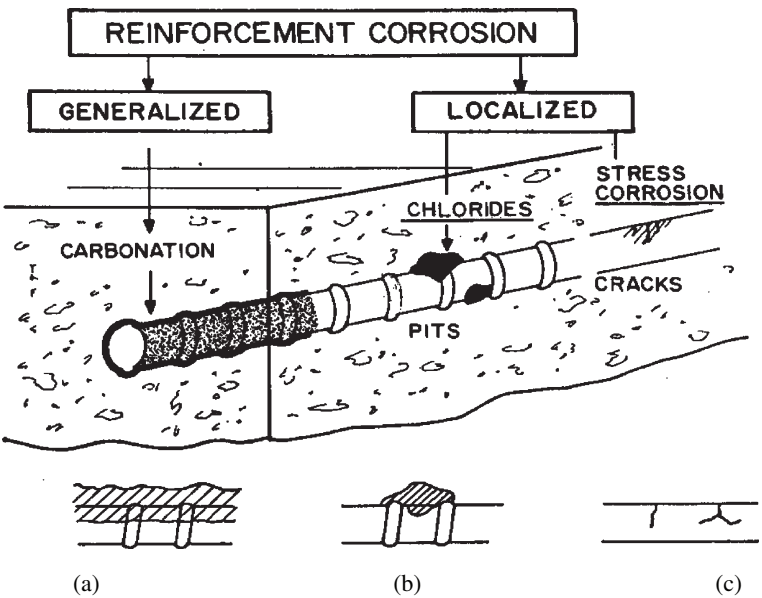

Figure 2: Types of corrosion of reinforcement: (a) carbonation, (b) chloride attack and (c) stress corrosion cracking.

1.2 Notions of electrochemical potential

Not all the metals have the same tendency to oxidize, that is, not all the metals are equally reactive. The activity of metals when in contact with an electrolyte can be expressed through Nernst equation:

$$E = E_0 + \frac{RT}{nF} \ln k, \tag{1}$$

where E is the actual potential, E_0 is the so-called 'standard potential', R is the gas constant, T is the absolute temperature, n is the number of electrons exchanged,

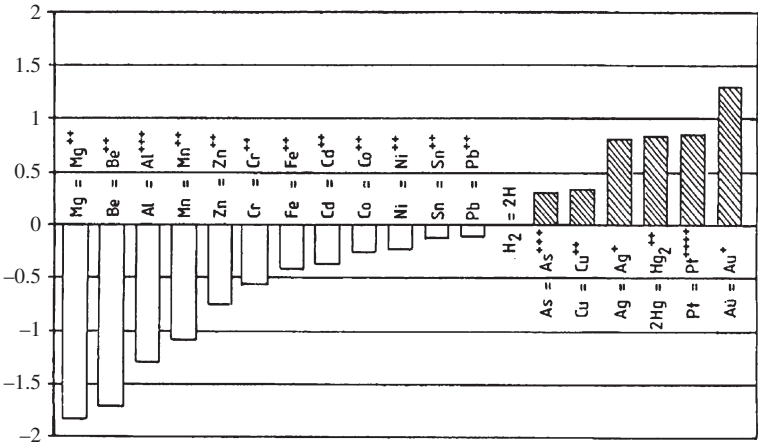

Figure 3: Nernst potentials shown in a graphic form. Positive values indicate noble metals and negative values indicate active ones.

F is the Faraday number and k is the equilibrium constant of the ions present in the electrolyte.

k takes different forms depending on the type of reaction. For the Fe(II)/Fe (metal) system, k is represented by the activity of the ion Fe^{2+} in the solution. Thus, if this activity is 10^{-3} mol/l, as $E_0 - 0.44$ V (SHE), the equilibrium potential E is [2]:

$$E_0 - 0.44 + \frac{0.059}{2}(-3) = 0.527 \text{ V}. \tag{2}$$

The potential is a measure of the facility of exchanging of electrons across the metal/electrolyte interface and of the ease of the reduction reaction. The absolute potential values cannot be determined and therefore they are given by comparison with a redox reaction (e.g. that of hydrogen in the third reaction) which is taken as reference. That is why corrosion potentials are expressed with reference to the hydrogen electrode, or to any other reference electrode (calomel, copper/copper sulphate, etc.). These electrodes have very rapid redox exchanges and therefore constant reference potentials. Figure 3 shows the values of the most common reference electrodes taken as 'zero', that of hydrogen electrode.

1.3 Pourbaix diagrams

The potential exhibited by an electrode in a particular electrolyte depends on a set of factors: (a) the standard potential of the anodic and cathodic reactions, (b) the temperature, and (c) the composition of the electrolyte, that is, its ionic concentration. The last factor is very well expressed by Pourbaix [3] using pH–potential diagrams (Fig. 4). These diagrams represent the conditions of potential and pH where a particular corrosion reaction is thermodynamically favourable (Nernst equation is used

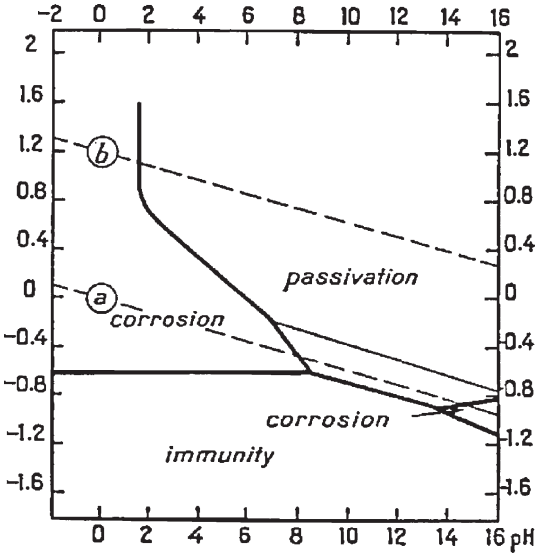

Figure 4: Pourbaix's diagram for Fe.

for the analysis of reactions). From the results the diagrams can be divided in three main zones: corrosion, passivity and immunity: The metals, when in contact with an aqueous solution may corrode, or become passive by the generation of a very stable oxide, or they may remain in a region of potentials where oxidation is not thermodynamically feasible (immunity).

Figure 4 shows Pourbaix's diagram for the Fe. The two lines a and b indicate the regions of water electrolysis. Below line b, water evolves to hydrogen gas and hydroxides: $2H_2O + 2e^- \rightarrow H_2 + 2OH^-$, and above line a, to oxygen and protons: $H_2O + 2e^- \rightarrow 2H^+ + O_2$.

1.4 Polarization

In spite of the usefulness of Pourbaix's diagrams, they represent only equilibrium conditions and therefore, kinetic aspects are not taken into consideration in them. Kinetic aspects have to be studied by following the changes in potential (overpotential) from equilibrium conditions (those indicated in Pourbaix's diagrams). Any change in potential from equilibrium conditions is due to the passage of a current and the phenomenon is called 'electrode polarization' [1, 4]. In general, it can be written as:

$$I = \frac{E_c - E_a}{R}, \tag{3}$$

where I is the current applied externally or recorded (if the change is induced in the potential), $E_c - E_a$ is the change in potential (overpotential or polarization) and R is the electrical resistance of the circuit.

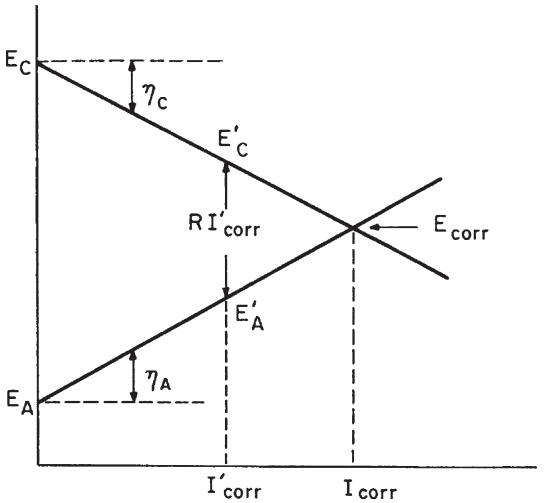

Figure 5: Evans diagram voltage/current for a corrosion cell in which the polarization curves have been linearized.

Although the relation between I and $(E_c - E_a)$ is generally not linear, Evans [1] introduced a simple representation which is used very much for the sake of illustration. Figure 5 depicts an Evans diagram. Evans diagrams helps to follow the evolution of the anodic, E_a, and cathodic, E_c, potentials with the passage of an external current, I. The slope of the lines represents the polarization, and their distance depends on the electrical resistance of the circuit, R.

A study of the types of polarization was carried out by Tafel in 1905 [4] to establish that for high enough polarization, the relation between the overpotential $\eta = E_c - E_a$ and the current is:

$$\eta = a + b \log i, \tag{4}$$

where a is the order at the origin and b is the slope. This expression enables the calculation of 'Tafel slopes', the basic parameter to study the kinetics of corrosion reactions, and the so-called 'polarization curves'.

1.5 Calculation of corrosion rate

It was in 1957 when Stern and Geary [5] in a study of the behaviour of polarization curves established that around the corrosion potential, i.e. when the current or overpotential is very small, the polarization curves could be linearized and therefore the slope of the curve (Fig. 6) is directly proportional to what was named 'polarization resistance', R_p:

$$\left(\frac{\Delta E}{\Delta I}\right)_{\Delta E \to 0} = R_p. \tag{5}$$

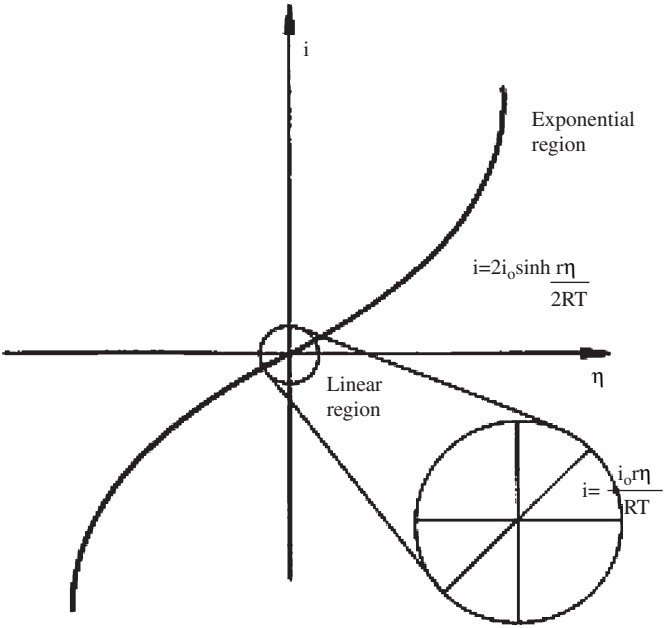

Figure 6: The polarization curve around the corrosion potential is linear and can be used to measure the polarization resistance, R_p. i = current density, i_0 = exchanged current, η = overpotential and $r = F$ = Faraday constant.

This resistance to polarization, determined by very small overpotentials, is inversely proportional to the corrosion current or rate through:

$$I_{corr} = B/R_p, \tag{6}$$

where B is a constant which is based on Tafel slopes (b_a, b_c):

$$B = \frac{b_a b_c}{2.3(b_a + b_c)}. \tag{7}$$

As the overpotentials needed to determine I_{corr} are very small, the results of the method are non-destructive. The technique has been much developed and is now the basis for the current determination of corrosion rates in many metal/electrolytes systems. It was applied to the study of reinforcement corrosion by Andrade and Gonzalez [6] in 1970 and has been implemented in corrosion-rate-meters for measuring in real-size structures by Feliú *et al*. [7].

2 Damage to structural concrete due to corrosion

The main factors leading to reinforcement corrosion are shown in Fig. 2: Carbonation induces a generalized corrosion while the presence of chloride ions in the

surroundings of the steel provokes localized corrosion. Stress corrosion cracking (SCC) has been detected in prestressing and post-tensioned structures [8].

2.1 Carbonation

Carbon dioxide is present in the air in proportions ranging from 0.03% to 0.1% depending on the local contamination. This gas reacts with the alkalinity of cement phases to give $CaCO_3$ as the main reaction product. This process leads into a decrease of the pH value of the pore solution from $pH > 13$ to $pH < 8$. At this neutral pH value, the passive layer of steel disappears and a general and uniform corrosion starts.

The CO_2, being a gas, penetrates through pore network of concrete. If the pores are filled with water, the gas dissolves in the liquid water and the penetration is then very slow (Fig. 7). If the pores are not saturated with water, then the CO_2 can easily penetrate by diffusion and reach internal parts of the concrete cover.

The carbonation reaction is then produced between the CO_2 gas and the alkaline ions present in the pore solution. Thus, in schematic form:

$$CO_2 + H_2O \rightarrow CO_3^{2-} + 2H^+$$

$$CO_3H_2 + \text{NaOH or KOH or } Ca(OH)_2 \rightarrow \begin{array}{l} Na_2CO_3 + H_2O \\ K_2CO_3 + H_2O \\ CaCO_3 + H_2O \end{array}$$

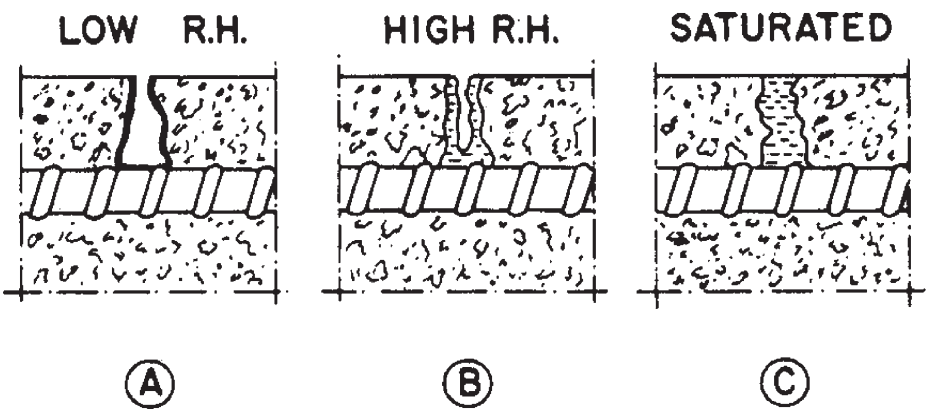

Figure 7: Simplified representation of the degree of saturation of concrete pores (RH, relative humidity). (A) CO_2 can easily penetrate, but the lack of moisture avoids carbonation. (B) Optimum moisture content for carbonation. (c) CO_2 penetrates very slowly when dissolving in water.

The neutralization of the pore solution, on the one hand, includes the leaching of Ca from the Ca-bearing cement phases, starting with C-S-H, and on the other, provokes the lowering of the pH of the pore solution.

Carbonation proceeds then in the water of the pore solution. If the concrete is very dry (Fig. 7), carbonation is not feasible due to the lack of water for the reaction to be produced. The maximum carbonation rate is noticed then at intermediate relative humidities (RHs) between 50% and 70% approximately. The oxides generated induce cracking of the cover through cracks parallel to the reinforcements (Fig. 8).

2.2 Chloride attack

The two main sources of chlorides for concrete structures are marine environments and the use of deicing salts in roads in cold climates. Chloride ions can be present in the concrete, either because they are introduced in the mixing materials, or because they penetrate from outside dissolved in the pore solution. While carbonation implies a gas that needs the pore network partially empty, chloride ions penetrate if the pores are filled with water, or a marine fog impregnates the concrete.

Figure 8: Crack pattern due to corrosion induced by carbonation.

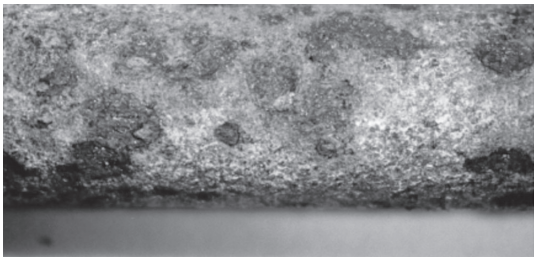

Figure 9: Localized attack due to chlorides.

Chlorides provoke a local disruption of the passive layer leading to localized attack (Fig. 9). The disruption is due to a local acidification induced by the protons liberated from the formation of iron hydroxides [4, 9]:

$$Fe^{2+} + 2H_2O \rightarrow Fe(OH)_2 + 2H^+$$

Depending upon the extension of the corrosion, cover cracking can appear or not. In submerged structures, cracking is often not induced.

2.2.1 Chloride threshold

For the attack to develop it is necessary that a certain amount of chlorides reach the steel surface. This amount is known as the chloride threshold and it is not an unique quantity because it is influenced by many parameters. The main influencing factors are:

- cement type: fineness, C_3A of cement, SO_3 content;
- presence of blending agents and their composition;
- curing and compaction;
- moisture content in concrete pores;
- steel type and surface finishing;
- local oxygen availability.

Too many parameters have prevented the identification of a single threshold value in the past [10]. More recent work [11] has, however, helped to identify the electrical potential as the controlling factor of the chloride threshold. Figure 10 shows the dependency. The same concrete induces different corrosion potentials, and this explains why the same concrete exhibits different chloride thresholds. The different corrosion potentials appear because of differences in the parameters listed above.

Figure 10 indicates that there is range of corrosion potentials (from around $-200\,mV_{SCE}$ to more noble potentials) in which the chloride threshold shows a minimum. When the potential is in a more negative/cathodic region, the amount of chloride ions inducing corrosion increases in coherence with the principles of cathodic protection [12]. Below a certain potential, the metal enters into the region of immunity of Pourbaix's diagram.

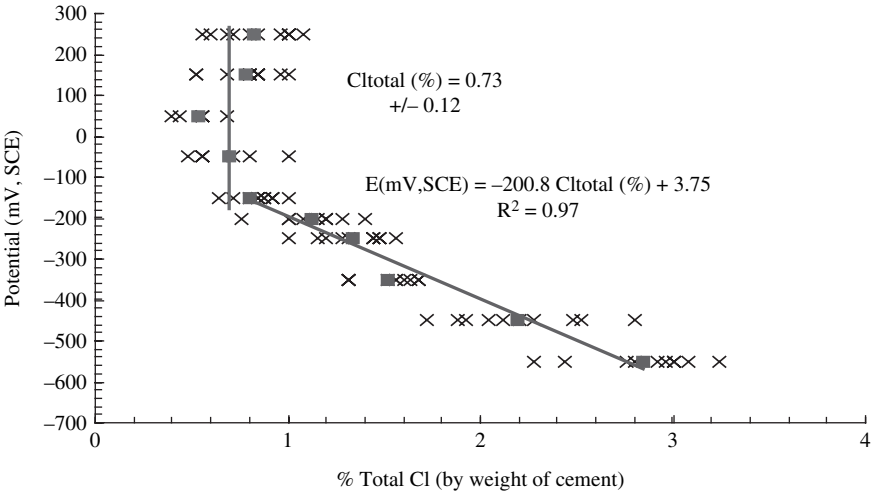

Figure 10: Dependence of chloride threshold on the potential.

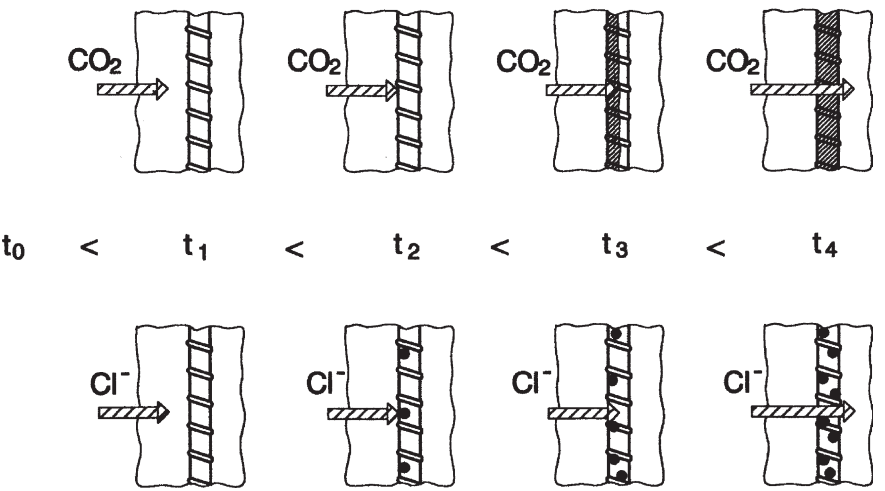

Figure 11: Progressive events of depassivation during carbonation and chloride penetration.

The usual chloride threshold specified in codes and standards is 0.4% by cement weight, not far from the minimum value obtained in the tests shown in Fig. 11, which was 0.7% by weight of cement.

The depassivation cannot be understood as an instantaneous process. Depassivation is a period of time during which the steel progressively becomes actively corroding (Fig. 11). Events of activity–passivity may develop during a long period without negligeable loss of steel cross-section being caused.

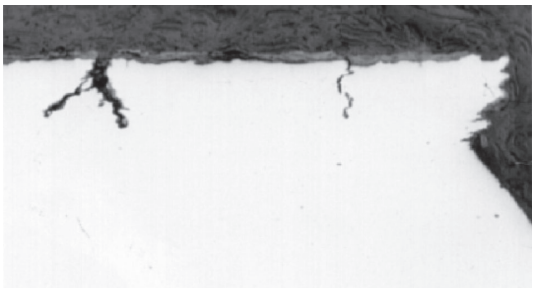

Figure 12: Cracks induced by a certain stress applied to a prestressing wire in bicarbonated solution.

2.2.2 Stress corrosion cracking

SCC is a particular case of localized corrosion. It occurs only in prestressing wires, when wires of high-yield point are stressed to a certain level and are in contact with a specific aggressive medium.

The process starts with the nucleation of microcracks at the surface of the steel (Fig. 12). One of the cracks may progress to a certain depth, resulting in a high crack velocity due to which the wire breaks in a brittle manner in relatively short time.

The mechanism of nucleation, and mainly of progression of SCC, is still subject to controversy. Nucleation can start in a surface non-homogeneity, spots of rust or inside a pit. The progression in enhanced by the generation of atomic hydrogen at the bottom of the crack. Of the several mechanisms proposed to explain the process, the one based on the concept of 'surface mobility' seems to best fit the experimental results. Surface mobility assumes that the progression of the crack is not of electrochemical nature but due to the mobility of atomic vacancies in the metal–electrolyte interface [13].

The only way to diagnose the occurrence of SCC is through the microscopic examination of the fractured surfaces in order to identify the brittle fracture. Thus, Fig. 13a shows a ductile fracture of a prestressing wire and Fig. 13b a brittle one (no striction is produced).

In the SCC phenomenon the metallographic nature and treatment of the steel plays a crucial role. Thus, quenched and tempered steels are very sensitive while the susceptibility of cold drawn steels is much lower. The use of the former is forbidden for prestressing in many countries.

2.3 Service life of reinforced concrete

When reinforced concrete started to be industrialized, it was believed that the material is going to have an unlimited durability. This is due to the supposition that cement alkalinity provides a chemical protection for the steel while the concrete cover is a physical barrier against contact with the atmosphere.

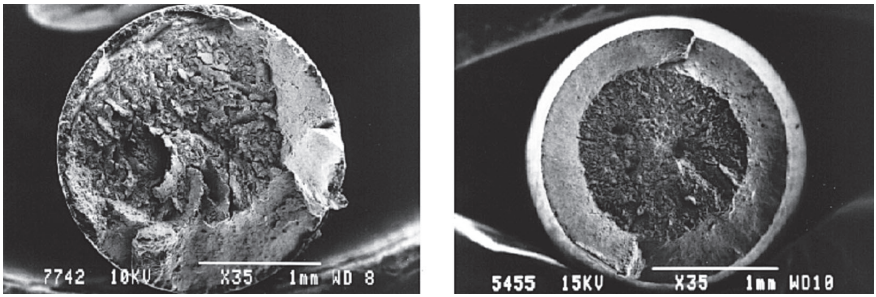

(a) (b)

Figure 13: Fracture of a prestressing wire: (a) brittle; (b) ductile.

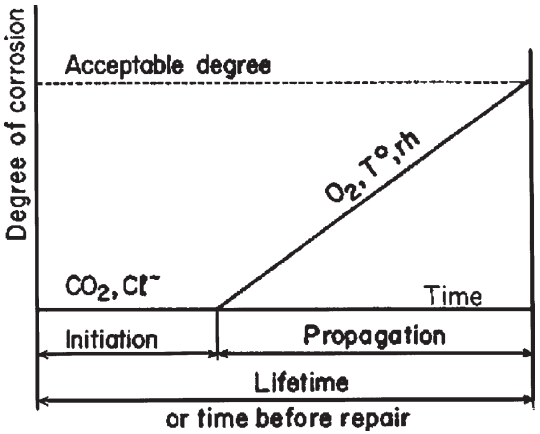

Figure 14: Service life model for reinforcement corrosion.

However, after 20–50 years of exposure to different environments, steel reinforcement exhibits corrosion, this being one of the most serious durability problems due to the economical consequences of repairs. Prediction of service life or time to corrosion has generated an increasing interest during the past two decades.

Judging the more or less theoretical proposals for service life prediction, such as that of ASTM E 632-81 until present situation, where concrete Codes and Standards try to incorporate durability chapters, it can be said that the most well-known service life model was the one published by Tuutti [14] in 1982. Figure 14 shows the model which specifies two periods for service life:

$$t_l = t_i + t_p. \tag{8}$$

Service life in this case is defined as t_l. The initiation period, t_i, comprises the time taken by the aggressive agents (chlorides or carbonation front to reach the reinforcement or passivate the steel). This is the relevant period if depassivation is

identified as the end of service life. However, if a certain amount of steel deterioration is considered as part of the design life, a period of propagation, t_p, can be considered until a certain 'unacceptable degree' of corrosion is reached.

This first proposal has been improved by other studies [15, 16]. The most common methodology followed at present when trying to design for reinforcement protection includes the following steps:

1. identification of aggressivity of the environment;
2. definition of the length, in years, of the service life, in addition to considering some special actions of maintenance or supplementary protection methods;
3. consideration of a calculation method for the attack progression;
4. specification of minimum concrete quality and cover depth.

2.3.1 Environmental aggressivity

Environmental actions are responsible for the lack of durability of reinforcement as they are the source of temperature cycles, of water supply through rain and snow, and of carbonation and chlorides. In general, no significant damage is noticed in indoor conditions, provided that no water is present due to leaking of pipes or lack of roof tightness.

Exposure classes are usually identified in Codes. Table 1 shows those specified in Eurocode 2 (CEN-1992 – part 1). In it, carbonation and chloride-containing ambients are separately considered.

2.3.2 Length of service life

In numerous standards, service life is defined as 'the period of time in which the structure maintains its design requirements of: safety, functionality and aesthetics without unexpected costs of maintenance'.

Services lives of 50–120 years are usually taken in relation to the types of structures. The explicit definition of length of service life has technical as well as legal implications, as civil responsibilities are involved for the designer and the constructor. Therefore, it should be considered as a reference period for the calculations, avoiding liabilities when these are not well specified.

2.3.3 Supplementary protection methods

In very aggressive environments or when the concrete element cannot have a sufficiently thick cover, supplementary protection methods should be specified from a design phase. The main methods are:

- cathodic protection,
- galvanized or stainless steel reinforcement,
- corrosion inhibitors,
- concrete coatings.

The main advantages and disadvantages of these methods are briefly outlined in Fig. 15 [17].

Table 1: Exposure classes in EN-206.

Class designation	Description of environment	Informative examples where exposure classes may occur
1. *No risk of corrosion or attack*		
X0	For concrete without reinforcement or embedded metal: all exposures except where there is freeze–thaw, abrasion or chemical attack For concrete with reinforcement or embedded metal: very dry	Concrete inside buildings with very low air humidity
2. *Corrosion induced by carbonation*		
Where concrete containing reinforcement or other embedded metal is exposed to air moisture, the exposure shall be classified as follows: Note: The moisture condition relates to that in the concrete cover to reinforcement or other embedded metal but, in many cases, conditions in the concrete cover can be taken as reflecting that in the surrounding environment. In these cases, the classification of the surrounding environment may be adequate. This may not be the case if there is a barrier between the concrete and its environment.		
XC1	Dry or permanently wet	Concrete inside buildings with low air humidity Concrete permanently submerged in water
XC2	Wet, rarely dry	Concrete surfaces subject to long-term water contact Many foundations
XC3	Moderate humidity	Concrete inside buildings with moderate or high air humidity External concrete sheltered from rain
XC4	Cyclic wet and dry	Concrete surfaces subject to water contact, not within exposure class XC2
3. *Corrosion induced by chlorides other than from sea water*		
XD1	Moderate humidity	Concrete surfaces exposed to airborne chlorides
XD2	Wet, rarely dry	Swimming pools Concrete exposed to industrial waters containing chlorides
XD3	Cyclic wet and dry	Parts of bridges exposed to spray containing chlorides Pavements Car parks
4. *Corrosion induced by chlorides from sea water*		
XS1	Exposed to airborne salt but not in direct contact with sea water	Structures near to or on the coast
XS2	Permanently submerged	Parts of marine structures
XS3	Tidal, splash and spray zones	Parts of marine structures

WIT Transactions on State of the Art in Science and Engineering, Vol 28, © 2007 WIT Press
www.witpress.com, ISSN 1755-8336 (on-line)

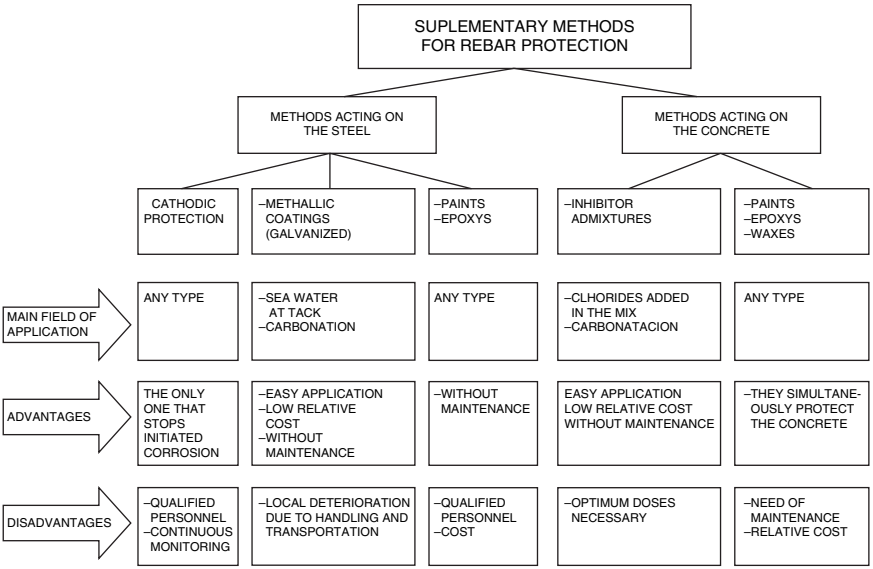

Figure 15: Supplementary methods of protection against reinforcement corrosion.

2.3.4 Calculation methods for attack penetration

The two main causes of corrosion, as previously described, are: the carbonation of concrete cover and the penetration of chloride ions.

Carbonation usually progresses by a diffusion mechanism while chlorides may penetrate also with a combination of absorption and diffusion (tidal or splash zones). Hydrostatic pressure may also lead into permeation. That is, among these three mechanisms, the most common are diffusion and absorption. They are known to follow the law of the 'square root of time':

$$x = K\sqrt{t}, \tag{9}$$

where x is the attack penetration depth (mm), t is the time (s) and K is a constant, depending on concrete and ambient characteristics. This square root law may be plotted on a log–log scale as shown in Fig. 16, and as suggested by Tuutti [14], which is very convenient and general.

2.3.4.1 Carbonation. It is known to be a consequence of the CO_2 gas penetration through water empty pores and its dissolution in the pore water followed by the reaction with the alkaline compounds present there. Calcium carbonates precipitates and the pH of the pore solution drops to values near neutrality. At these neutral pH the steel depassivates and starts to corrode.

The *carbonation* rate has been modelled by many researchers, although only three models will be commented. Those are the models proposed by Tuutti [14],

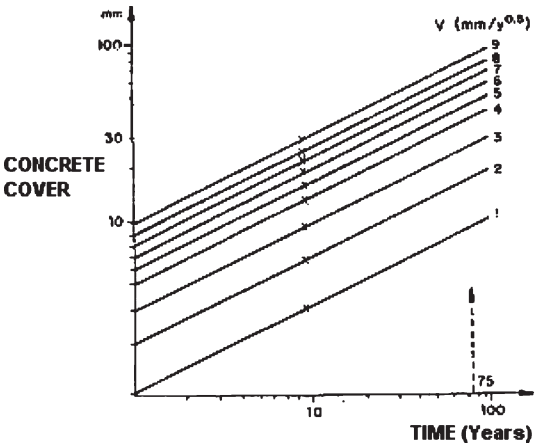

Figure 16: Representation of the square root law in log–log diagrams. The numbers corresponding to the parallel lines of slope 0.5 represent the values of the constant K.

Bakker [18] and Parrott [19]. The three models have the concrete requirements and climatic (humidity) loads as input factors.

Tuutti [14] based his method on the known diffusion theory of 'moving boundaries', which offers the following expression for the calculation of the rate of advance of the carbonation front:

$$\frac{C_s}{C_x} = \sqrt{\pi}\left[\frac{x/\sqrt{t}}{2\sqrt{D}}\right]\exp\left[\frac{x^2}{4Dt}\right]\operatorname{erf}\left(\frac{x/\sqrt{t}}{2\sqrt{D}}\right), \tag{10}$$

where C_s is the CO_2 concentration in the atmosphere (mol/kg), C_x is the amount of bound CO_2 (cement phases plus pore solution) (mol/kg), D is the CO_2 diffusion coefficient (m^2/s), x is the carbonation depth (mm) and t is the time (s).

Bakker [18] based his proposal on a diffusion solution of the first order, but taking into account the internal moisture content of the concrete due to the RH cycling. This leads to the introduction of the concept of 'effective time' of action of the carbonation, as it is known that carbonation cannot progress in wet concrete. The expression reached is:

$$x_n = \sqrt{\frac{2D_c}{a}(C_1 - C_2)\left[t_{d1} + t_{d2}\left(\frac{x_1}{B}\right)^2 + t_{d3}\left(\frac{x_2}{B}\right)^2 + L + t_{dn}\left(\frac{x_{n-1}}{B}\right)^2\right]}, \tag{11}$$

where

$$B = \sqrt{\frac{2D_v}{b}(C_3 - C_4)}, \tag{12}$$

$t_{d1}, \ldots, t_{dn}$ are the times of test, x_i is the carbonation depth (mm), a is the CaO content in the cementitious materials (mol/kg), b is the amount of water which

evaporates from concrete (kg/m^3), D_c is the diffusion coefficient of CO_2 at a particular RH in concrete (m^2/s), D_v is the diffusion coefficient of water vapour at a particular RH in concrete (m^2/s), $C_1 - C_2$ is the difference of CO_2 concentration between air and concrete (mol/kg) and $C_3 - C_4$ is the difference in RH between air and concrete (mol/kg).

Parrott [19] followed a different approach offering an empirical solution based on the gas permeability of the concrete. Thus, he obtained an 'empiric expression' by mathematical fitting of carbonation depths measured in real structures. His fitting considers the 95% confidence range and the expression reached in function of the gas permeability is:

$$x = 64\frac{k^{0.4}t^{0.5}}{c^{0.5}}, \tag{13}$$

where x is the carbonation depth (mm), k is the oxygen permeability coefficient (m^2/s), t is the time (years) and c is the CaO content in the cement (mol/kg).

When applying eqns (10–13) to real data obtained from carbonated concrete, they give very similar results, as shown in Fig. 17. The choice of preference depends on the available input data.

2.3.4.2 Chloride penetration rates. Chloride ingress through concrete cover can occur in marine or salty environments. When the chlorides arrive to the reinforcement in a certain quantity, local rupture of the passive layer is produced and corrosion starts. The process of penetration can be modelled as a pure diffusion process or by the square root law where V is the chloride penetration rate V_{Cl} [20]. In this case, the threshold of chlorides has to be pre-established as a front (Fig. 18) whose advance indicates the penetration depth of chlorides inducing corrosion. Plots similar to Fig. 17 can be then used.

For modelling chloride ingress other expressions based on Fick's second law are however more used. The solution more known is based on assumption of a semi-infinite media with a constant surface concentration, C_s [21].

$$C_x = C_s\left[1 - \text{erf}\frac{x}{2\sqrt{Dt}}\right], \tag{14}$$

where C_x is the chloride concentration at the depth x and time t and D is a non-steady state diffusion coefficient.

The current practice applies this equation to specimens tested in the laboratory in contact with a pond filled with NaCl solution (Fig. 19) or in cores drilled from real structures located in marine environments or in contact with deicing salts.

In the specimens or cores, slides are cut or ground parallel to the surface in contact with the chlorides. The equation is fitted, as Fig. 20 shows, to the graph of chloride concentration–penetration depth. By this fitting, the values of D and C_s are obtained. The values of D are then used to predict further evolution of the chloride profile. At this respect it has to be taken into account that, as chlorides react with the aluminates of the cement paste, the process is slower than a pure diffusion or absorption. And the Diffusion coefficient has to consider the amount

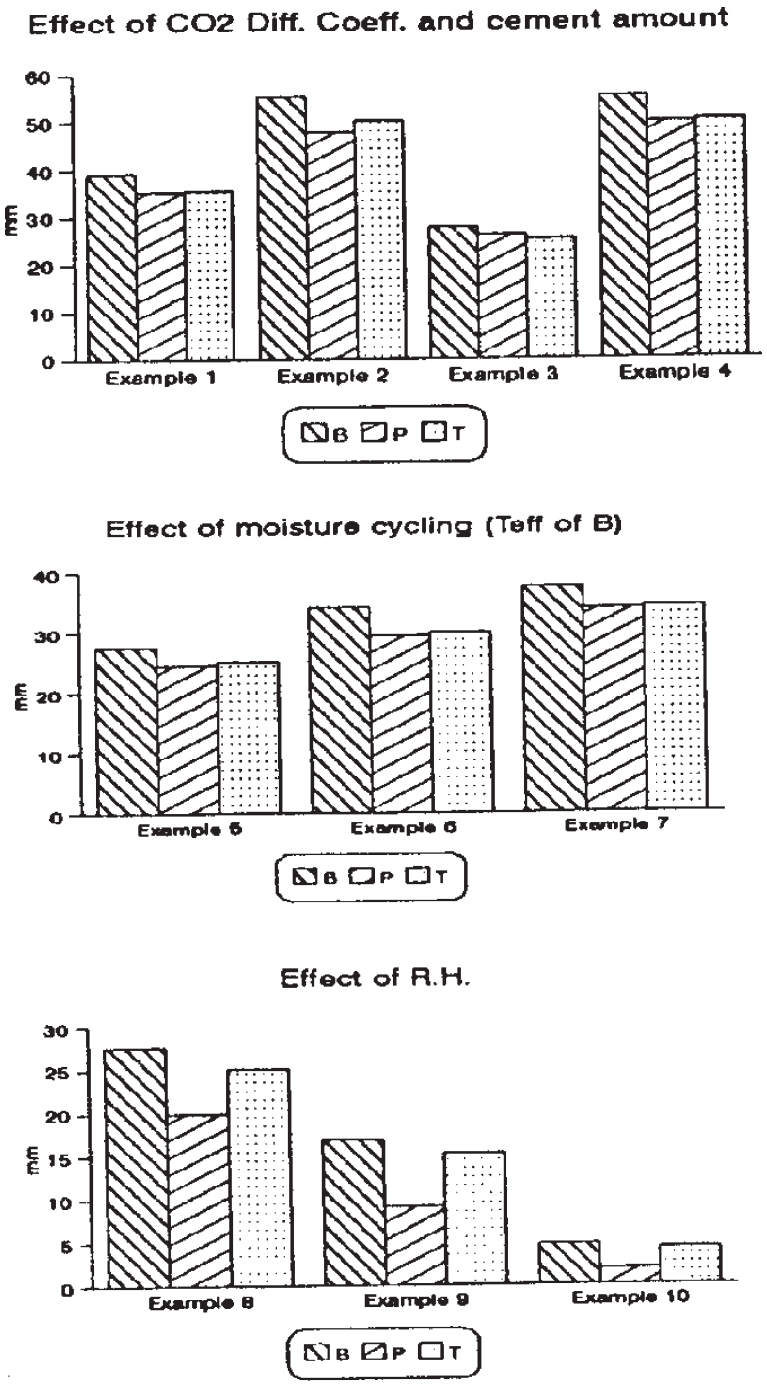

Figure 17: Carbonation depth results in concrete specimens obtained by means of the formulae proposed by Bakker (B), Parrot (P) and Tuutti (T) for the carbonation rate.

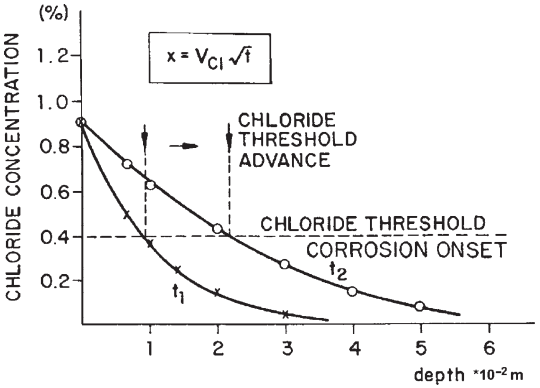

Figure 18: Definition of a chloride threshold enables to apply the square root law to chloride profiles. V_{Cl} = chloride penetration rate.

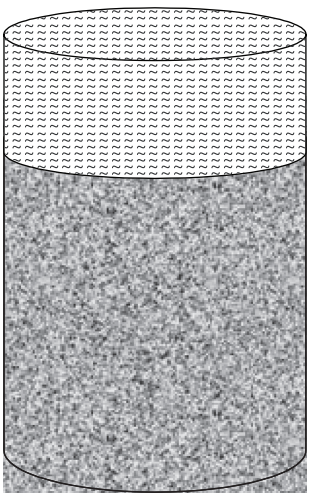

Figure 19: Typical concrete specimen with a pond containing a chloride solution in order to test the chloride diffusion coefficient.

of reacted or bound chlorides. In general, diffusion and reaction are not separated and an "Apparent D, D_{ap}" is used. Then in the following $D = D_{ap}$.

In spite of the general use of this model, it fails in many observations in real structures as its initial and boundary conditions are not fulfilled in many real environments. The main difficulties for its application are [22]:

- C_s does not remain constant and as the D value depends on it, both parameters should be given together. Thus, Fig. 21 shows two profiles (B and C) with different C_s but the same C_x at x in the rebar surface. B exhibits an apparent D

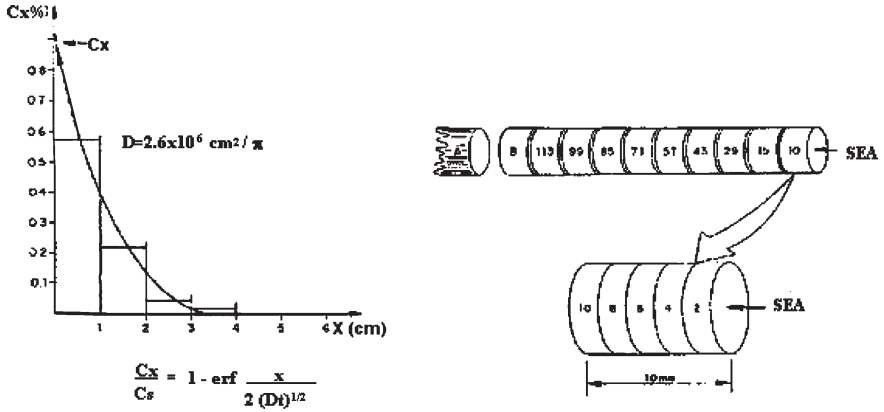

Figure 20: Fitting of the solution of Fick's second law to a chloride profile in order to obtain the diffusion coefficient and the surface concentration.

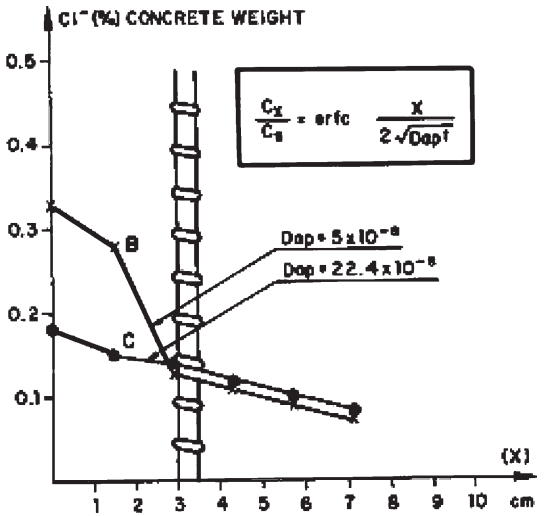

Figure 21: Two chloride profiles which indicate that the diffusion coefficient may be a misleading parameter. D_{ap} = apparent coefficient diffusion.

lower than that of C while both have the same risk for the reinforcement or even B supposes a higher one due to the higher total amount of chlorides.

- The D value is variable as well. It seems to decrease: with time, with higher external concentrations and with lowers temperatures. A time dependence of t has been introduced through [23]:

$$D(t) = D(t_0)\left[\frac{t}{t_0}\right]^n \tag{15}$$

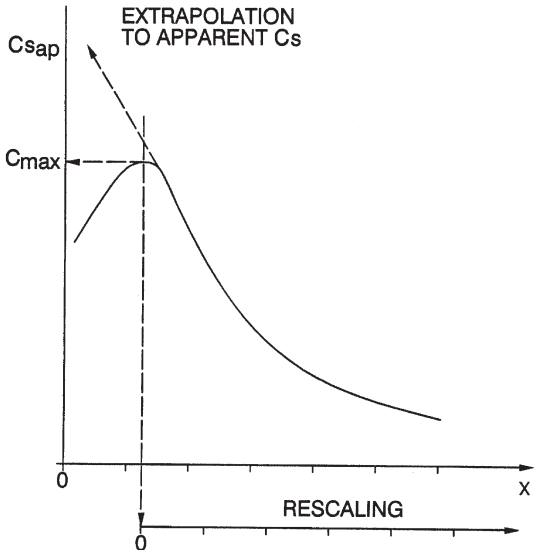

Figure 22: Pattern of chloride profiles showing a maximum beyond concrete surface. $C_{s\,ap}$ = apparent surface concentration.

where t_0 is the initial time, t is any time and n is an exponent of value around 0.5. Although the predictions made with this time dependence are not so unrealistic, the power n is so predominant that neglects any other influence.

- The error function equation does not take into account any mechanism other than diffusion, when absorption is also of very great importance in many real environments. In fact, the skin of the concrete surface behaves usually different than concrete bulk due to: (a) the direct contact with environment developing gradients of moisture from outside to the concrete interior; (b) its usual different composition with higher amount of paste and mortar and therefore higher porosity compared with the interior; and (c) the progressive carbonation in the cases where it occurs. The skin of the concrete then may exhibit a different D value than the interior modifying the profile and showing a maximum in the chloride concentration as the figure indicates. Also wet and dry regimes can lead into similar shapes of chloride profiles. The solution of this type of profile has been modelled through a 'skin effect' [24] although the D value can be also obtaining by rescaling the depth axis to placing the 'zero' at the maximum which would be C_s (Fig. 22).

2.3.5 The maximum tolerable amount of corrosion

Regarding the *maximum tolerable amount* of corrosion (loss of cross section of bars or "attack penetration", P_x) [14] in the case of new structures, both carbonation and chloride attack have to be considered separately. While in the case of carbonation a certain propagation period can be considered as part of the design service life

(as the expected corrosion is homogeneous), almost no propagation period should be considered in the case of localised attack due to chlorides. This is because the uncertainties linked to how much localised and deep the corrosion pits may be do not enable at present the acceptance of such a risk from the design phase of the structure.

With regard to a limit for the case of the carbonation attack, a general suggestion is to accept a corrosion penetration depth of about 100–200 μm. Assuming a corrosion rate of about 5 μm/year, this would aim at propagation periods of 20–40 years [25]:

$$t_l = \text{service life} = t_i + t_p = K_c\sqrt{t} + \frac{PL}{CR}, \tag{16}$$

where t_i is the corrosion initiation time (years), t_p is the corrosion propagation time (years), K_c is the carbonation coefficient, PL is the penetration limit (mm) and CR is the corrosion rate (I_{corr}, μm/year).

In the case of chlorides, the local attack may result in a very significant cross-section loss without negligible loss of metal. If the pits are very localized, the maximum propagation period to be considered should be 5–10 years [25].

2.3.6 Propagation period

When the reinforcement starts to corrode, several damages occur. The four main consequences of corrosion are illustrated in Fig. 23: (a) a loss of steel cross section due to the penetration of corrosion attack; (b) a loss in steel ductility due to the embrittlement caused by the corrosion inducing local acidification at the steel–concrete interface; (c) loss of steel–concrete bond due to the reduction of bar cross-section and the generation of iron oxides; and (d) cracking of concrete cover due to the pressure resulting from the production of oxides of higher volume than the parent steel [25, 26].

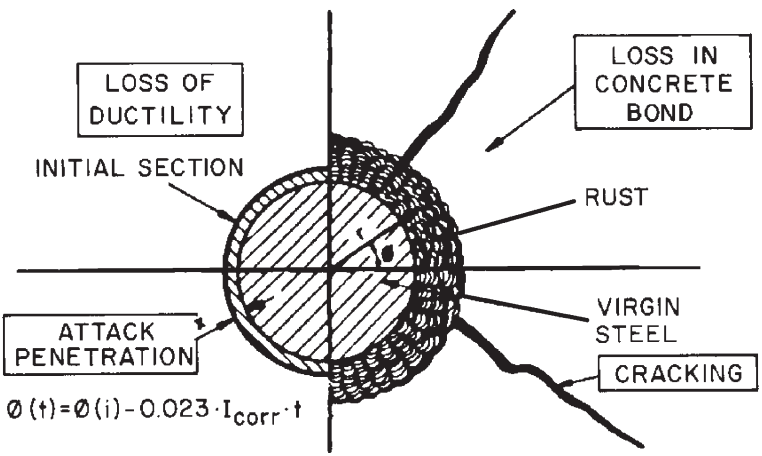

Figure 23: Consequences of reinforcement corrosion leading to loss of load-bearing capacity.

These damages affect to the load-bearing capacity of the whole structure and, in consequence, compromise the aesthetics, serviceability and safety, that is, the durability inherent to reinforced concrete as a construction material.

2.3.6.1 Detailed assessment of concrete structures affected by rebar corrosion. The main objective of a structural assessment is the residual safety level determination, in order to establish an adequate intervention programme with the higher degree of available information. On the other hand, a structural assessment can also be used for calibration of more simplified methodologies [26–28].

The three main aspects to be analysed in a structural assessment are:

- action, or better action effect, evaluated on the structure;
- deterioration process evaluation;
- safety or serviceability limit states verification.

The last two aspects will be explained below for structures affected by reinforcement corrosion:

Deterioration process evaluation. The attack by corrosion will be appraised by using a *penetration attack*, P_x, which is the loss of reinforcement radius. P_x is the main parameter that will allow a correlation with the general effects previously mentioned on the composite concrete–steel section [25]. This parameter can be measured visually from the residual diameter or estimated by means the corrosion rate I_{corr}.

P_x is related to I_{corr} by the expression:

$$P_x[\text{mm}] = 0.0116\alpha I_{\text{corr}} t, \tag{17}$$

where t is the time and α is the pitting factor which takes into account the type of corrosion (homogeneous or localised) [29, 30].

The determination of I_{corr} in real structures will depend on several factors, and several strategies may be used for its determination in order to obtain a *representative value* of the loss of diameter P_x [28]:

- Several measurements at different times in different environmental conditions, to obtain a mean value to be used in the calculation; this can be achieved by using embedded sensors.
- A single value which is averaged with I_{corr} values obtained in a drilled core submitted in the lab to water saturation.
- The use a classification of exposure classes where representative corrosion values are proposed.

Reinforcement corrosion provokes on concrete–steel sections the effects shown in Fig. 23. These effects are related to the P_x value according the following principles:

Effective steel section reduction: Depending on the type of aggressive medium and the type of corrosion, their influence on the effective steel cross section is quite

Table 2: β values for crack width evolution. Characteristic values.

	Top rebars	Bottom rebars
β	0.01	0.0125

different [25]. Thus, $\alpha = 2$ in eqn (17) if the corrosion is homogeneous and $\alpha = 10$ for very localized chloride-induced corrosion [28]. The calculation of the rebar diameter can be achieved through:

$$\Phi_{\text{Res}} = \Phi_0 - P_x = \Phi_0 - 0.0116\alpha I_{\text{corr}} t, \tag{18}$$

where Φ_{Res} is the residual diameter and Φ_0 is the initial diameter.

Cover cracking: The oxides generated in the corrosion process provoke a tensional state in the concrete cover that will produce cover cracks of different widths, w, reducing consequently the cross-section of the concrete element and therefore their load-bearing capacity [31]. Several empirical expressions have been developed that can evaluate the crack width of the cover as a direct function of the corrosion attack P_x, and several geometric and mechanical parameters. The expression that is suggested is:

$$w[\text{mm}] = 0.05 + \beta[P_x - P_{x0}] \quad [w < 1\,\text{mm}]. \tag{19}$$

The value of P_{x0} depends mainly on the concrete cover/rebar diameter ratio, C/Φ, and the tensile strength of the concrete $f_{\text{Ct,sp}}$. Equation (24) provides an estimation of P_{x0}:

$$P_{x0} = 83.8 \times 10^{-3} + 7.4 \times 10^{-3} \left(\frac{C}{\Phi}\right) - 22.6 \times 10^{-3} f_{\text{Ct,sp}}, \tag{20}$$

where β depends on the rebar position in the element according to Table 2.

Loss of bond: The concrete–steel bond is the responsible of the composite behaviour of both materials [28]. However, corrosion provokes a reduction in bond due to the cover cracking and stirrups corrosion. Finally a limit state of bond can be achieved. Three main aspects are considered:

Residual bond assessment: Table 3 shows empirical expressions obtained based on several tests that allow the determination of realistic residual bond values. All of them depend on the attack penetration P_x.

For intermediate cases where the amount of stirrups is low, below the actual minimum, or the capacity of stirrups is strongly reduced by the corrosion effect,

Table 3: Relationship between P_x and residual bond strength f_b (MPa). Characteristic values.

With stirrups	No stirrups
$f_b = 4.75 - 4.64\,P_x$	$f_b = 2.50 - 6.62\,P_x$

Table 4: Bond strength values, intermediate amount of stirrups. Characteristic values.

f_b	$10.04 + m(1.14 + P_x)$
m	$-6.62 + 1.98(\rho/0.25)$
ρ	$n[(\phi_w - \alpha \boldsymbol{P}x)/\phi]^2$

Where ϕ is the initial longitudinal diameter (mm), ϕ_w is the transversal diameter (mm), n is the number of transversal reinforcements, α is the coefficient that depends on the type of corrosion, m is the adjust parameter and ρ reinforcement ratio.

the expressions in Table 4 may be applied. These expressions are applied for P_x values between 0.05 and 1 mm with $\rho \leq 0.25$.

Influence of external pressures that can be present due to external supports: Thus, expressions similar to that presented in Eurocode 2 have been developed:

$$f_b = \frac{(4.75 - 4.64P_x)}{1 - 0.098p}, \tag{21}$$

where f_b is the bond strength (MPa), P_x is the corrosion attack (mm) and p is the external pressure in the bond zone (MPa). This expression can be used for the bond strength evaluation of the rebar at element ends.

Figure 24 shows an application of these expressions in a reinforcing bar diameter of 20 mm without stirrups (curve 3) or with $4\phi 8$ stirrups. Curves 1 and 2 correspond to the bond reduction with a reduction at the end of the element without pressure (1 with homogeneous corrosion and 2 with pitting corrosion), curve 4 corresponds to an external force of 5 MPa.

Relationship between bond and crack width: Several expressions have been developed for relating the residual bond with the crack width (Table 5).

Rebar ductility: Several tests of corroded rebars have shown an important reduction in the rebar ductility not only in the final strain of the rebar but also in the strain–stress curve of the corroded rebar. The tests show that the yield point is

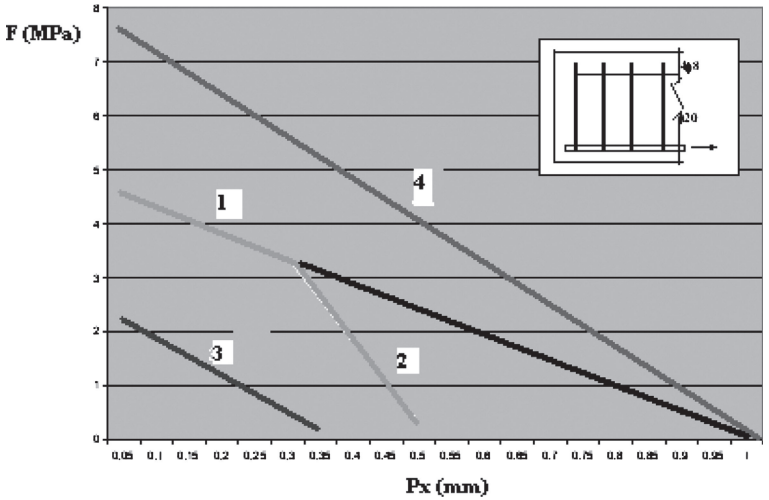

Figure 24: Loss of bond as a function of P_x (in mm). (1) Element with stirrups without pits; (2) element with pits in stirrups; (3) element without stirrups; (4) element with stirrups and external pressure.

Table 5: Relationship between residual bond strength f_b (MPa) and crack width w (mm). Characteristic values.

Stirrups	No stirrups
$f_b = 4.66 - 0.95w$	$f_b = 2.47 - 1.58w$

diffuse and the final strain is considerably reduced. However, in all cases the final value of the ultimate strain is above 1% which is the value to be used in Ultimate Limit State.

Structural analysis. The structural analysis can be carried out following the main principles of structures with linear–elastic analysis. It is important to identify the presence of cracks in sections produced by corrosion or not in order to reduce their stiffness in the structural model.

Limit state verification. *Ultimate limit state:* For slab and beams, a conservative value of the ultimate bending moment can be calculated by using the classical models adding correction in order to take into account the reduced steel section and the concrete section spalled [28]. A possible reduction due to bond deterioration as a result of corrosion should be considered, especially if the corrosion attack is on the tensile zone of the beams.

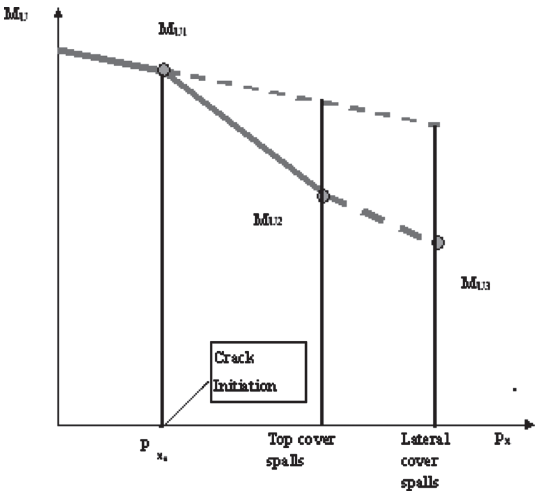

Figure 25: Time–history evolution of ultimate bending moment.

Although shear and bending moment are assumed to have the same safety in the design phase for beams without corrosion because the shear formulation is considered to be conservative, several factors may induce a premature failure of shear for corroded beams, such as:

- small diameters on stirrups,
- lower cover for stirrups,
- spalling of cover.

In order to check the ultimate axial effort of a column element, the reduction should be applied on the concrete section in the case of spalling, and if there are no stirrups, on the longitudinal bars subjected to compression due to risk of buckling.

Although no tests have been performed regarding punching shear it is possible to extrapolate the shear test to slabs in order to use a verification procedure for punching in slabs.

The time–history evolution of the load-bearing capacity is simplified by using a linear interpolation between the crack initiation and the spalling point of lateral and top covers. It can be proved that, for normal concrete sections the exact calculation (step by step) provide a negligible error using this simplification. Thus, it is necessary to calculate three points in Fig. 25. The ultimate section effort (M_{U1} in the example) at the crack initiation point P_{x0}, the ultimate section effort (M_{U2}) when the top cover spalled (it is assumed that the top cover can be neglected when the crack width at top is >0.2 mm), and finally (M_{U3}) when the lateral cover spalls (the same criteria applies).

Serviceability limit state: The serviceability limit states to be checked should be [28]:

- exterior aspect of the structures (rust, spalling);
- cracking of the cover due to corrosion or excessive loading;
- excessive deflections.

For the deflection and crack checking due to loading, the expressions provided by Eurocode 2 can be used, reducing the steel section, the spalled concrete and the cracking if it exists. However, it is the owner of the structure who has to establish their acceptable degree for their structures regarding serviceability conditions.

3 Final remarks

Reinforced concrete is the most widely used construction material. Cement consumption ranges from 0.2 to 1 tonne per person, which means 1.4–7 tonnes of concrete per person. With more than a century of experience, it is now known that it performs adequately in very diverse climates and moderately aggressive environments [32].

However, for very long life, beyond 75 years, or standing up to very aggressive environments, reinforced concrete needs a minimum quality and cover thickness, or even supplementary protection methods to avoid reinforcement corrosion.

In sum, concrete structures should be designed with a specified maintenance regime and periodically inspected in order to lengthen their service life. Management tools are being developed to help the owners to protect their structures and contribute to reduce repair costs.

Nomenclature

E	actual potential
E_0	standard potential
R	gas constant
T	absolute temperature
e^-	electrons exchanged
k	equilibrium constant
I	current applied or recorded
i_0	exchanged current
η	change in potential, overpotential ($E_c - E_a$)
R	electrical resistance
E_a	anodic potential
E_c	cathodic potential
R_p	polarization resistance
B	constant based on Tafel slopes
b_a	anodic Tafel slope
b_c	cathodic Tafel slope
t_l	service life
t_i	initiation period
t_p	propagation period

x	attack penetration depth
t	time
K	constant depending on concrete and ambient characteristics
C_s	CO_2 concentration in the atmosphere
C_x	amount of bound CO_2
D	CO_2 diffusion coefficient
D_c	diffusion coefficient of CO_2 at a particular RH in concrete
D_v	diffusion coefficient of water vapour at a particular RH in concrete
t_d	time of test
a	CaO content in cementitious materials (Bakker model)
b	amount of water which evaporates from concrete
$C_1 - C_2$	difference of CO_2 concentration between air and concrete
$C_3 - C_4$	difference in RH between air and concrete
c	CaO content in cementitious materials (Parrott model)
V_{Cl}	chloride penetration rate
D	non-steady state diffusion coefficient
t_0	initial time
K	carbonation coefficient
PL	penetration limit
or I_{corr}	corrosion rate (CR)
P_x	penetration of attack
α	pitting factor
Φ_{Res}	residual diameter
Φ_0	initial diameter
$f_{Ct,sp}$	tensile strength of the concrete
w	crack width
β	parameter for the estimation of crack width that depends of the rebar position
f_b	residual bond strength
ϕ	initial longitudinal diameter in mm
ϕ_w	transversal diameter in mm
n	number of transversal reinforcements
α	coefficient that depends on the type of corrosion
m	adjust parameter
ρ	reinforcement ratio
p	the external pressure in the bond zone

References

[1] Evans, U.R., *The Corrosion and Oxidation of Metals*, Arnold and Co.: London, 1960.

[2] Tomashov, N.D., *Theory of Corrosion and Protection of Metals*, Macmillan Co.: New York, 1966.

[3] Pourbaix, M., *Atlas of Electrochemical Equilibria in Aqueous Solutions*, NACE: Houston, TX, 1974.

[4] Uhlig, H.H., *Corrosion and Corrosion Control*, Wiley and Sons: New York, 1971.
[5] Stern, M. & Geary, A.L., Electrochemical polarization. A theoretical analysis of the shape of polarization curves. *Journal of the Electrochemical Society*, **104(1)**, pp. 56–63, 1957.
[6] Andrade, C. & Gonzalez, J.A., Quantitative measurements of corrosion rate of reinforcing steels embedded in concrete using polarization resistance measurements. *Werkst. Korros.*, **29**, p. 515, 1978.
[7] Feliú, S., González, J.A., Feliú, S., Jr. & Andrade, C., Confinement of the electrical signal for in situ measurement of polarisation resistance in reinforced concrete. *ACI Materials Journal*, September–October, pp. 457–460, 1990.
[8] Slater, J.E., *Corrosion of Metals in Association with Concrete*, ASTM STP-818, ASTM: Philadelphia, PA, 1983.
[9] Hoar, T.P., Passivity, passivation, breakdown and pitting. *Corrosion*, Vol. 1, ed. L.L. Shreir, Butterworths: London, 1978.
[10] Hausman, D.A., Criteria of cathodic protection of steel in concrete. *24th Conf. of NACE*, Cleveland, OH, 1968.
[11] Alonso, C., Castellote, M. & Andrade, C., Chloride threshold dependence of pitting potential of reinforcements. *Electroquimica Acta*, **47**, pp. 3469–3481, 2002.
[12] Pedeferri, P., *Corrosione e protezione dei materially metallici*, Clup.: Milano, 1981.
[13] Galvele, J., A stress corrosion cracking mechanism based on surface mobility. *Corrosion Science*, **27**, pp. 1–3, 1987.
[14] Tuutti, K., *Corrosion of Steel in Concrete*, CBI Research Report 4:82, Swedish Cement and Concrete Research Institute: Stockholm, 1982.
[15] Gjorv, O.E. & Vennesland, O., Diffusion of chloride ions from seawater into concrete. *Cement and Concrete Research*, **9**, pp. 229–238, 1979.
[16] Page, C.L., Short, N.R. & El Tarras, A., Diffusion of chloride ions in hardened cement pastes. *Cement and Concrete Research*, **11**, pp. 395–406, 1981.
[17] Andrade, C. & Alonso, C., Progress on design and residual life calculation with regard to rebar corrosion of reinforced concrete. *Techniques to Assess the Corrosion Activity of Steel Reinforced Concrete Structures*, ASTM STP-1276, eds. N. Berke, E. Escalante, C.K. Nmai & D. Whiting, pp. 23–40, 1996.
[18] Bakker, R., Prediction of service life reinforcement in concrete under different climatic conditions at a given cover. *Int. Conference on Corrosion and Corrosion Protection of Steel in Concrete*, Sheffield, UK, ed. R.N. Swamy, 1994.
[19] Parrott, L.J., Design for avoiding damage due to carbonation-induced corrosion – ACI-SP-145-15. *Int. ACI/CANMET Conference of Durability of Concrete*, Nice, France, ed. M. Malhotra, pp. 283–298, 1994.

[20] Andrade, C., Sagrera, J.L. & Sanjuán, M.A., Several years study on chloride penetration into concrete exposed to Atlantic Ocean water. *2nd Rilem Workshop of Testing and Modelling Chloride Penetration into Concrete*, Paris, 2000.

[21] Collepardi, M., Marcialis, A. & Turriziani, R., Penetration of chloride ions into cement pastes and concretes. *Journal of the American Ceramic Society*, **55**, pp. 534–535, 1972.

[22] Andrade, C., Díez, J.M., Alonso, C. & Sagrera, J.L., Prediction of time to rebar initiation by chlorides: non-Fickian behaviour of concrete cover. *Concrete in the Service of Mankind*, eds. R.K. Dhir & P.C. Hewlett, E & FN Spon: London, pp. 455–464, 1996.

[23] Mangat, P.S. & Molloy, B.T., Prediction of long term chloride concentration in concrete. *Materials and Structures*, **27**, pp. 338–346, 1994.

[24] Andrade, C., Díez, J.M. & Alonso, C., Mathematical modelling of a concrete surface 'skin effect' on diffusion in chloride contaminated media. *Advanced Cement Based Materials*, **6**, pp. 39–44, 1997.

[25] Andrade, C., Alonso, C. & Rodriguez, J., Remaining service life of corroding structures. *IABSE Symposium on Durability*, Lisbon, September, pp. 359–363, 1989.

[26] Rodriguez, J., Ortega, L.M. & García, A.M., Assessment of structural elements with corroded reinforcements. *Int. Conference on Corrosion and Corrosion Protection of Steel in Concrete*, Sheffield, UK, ed. R.N. Swamy, pp. 171–185, 1994.

[27] Rodriguez, J., Ortega, L.M., Casal, J. & Díez, J.M., Assessing the structural condition of concrete structures with corroded reinforcements. *International Congress on Concrete in the Service of Mankind*, Dundee, UK, Vol. 5, June, eds. R. Dhir and P.C. Hewlett, 1996.

[28] Rodriguez, J., Andrade, C., Izquierdo, D. & Aragoncillo, J., Manual of assessment of structures affected by reinforcement corrosion, EU Project Contecvet IN309021, http://www.ietcc.csic.es/

[29] González, J.A., Andrade, C., Alonso, C. & Feliú, S., Comparison of rates of general corrosion and maximum pitting penetration on concrete embedded steel reinforcement. *Cement and Concrete Research*, **25(2)**, pp. 257–264, 1995.

[30] Andrade, C. & Arteaga, A., *Statistical Quantification of the Propagation Period*, Internal report Brite/Euram BE95-1347, Duracrete, 1998.

[31] Alonso, C., Andrade, C., Rodríguez, J. & Díez, J.M., Factors controlling cracking of concrete affected by reinforcement corrosion. *Materials and Structures*, **31**, pp. 435–441, 1998.

[32] Andrade, C., Alonso, C. & Sarría, J., Corrosion rate evolution in concrete structures exposed to the atmosphere. *Cement and Concrete Composites*, **24**, pp. 55–64, 2002.